Engineering TM1459 for Stabilisation against Inactivation by Amino Acid Oxidation

Birgit Grill, Tea Pavkov-Keller, Christoph Grininger, Barbara Darnhofer, Karl Gruber, Mélanie Hall, Helmut Schwab*, and Kerstin Steiner*

DOI: 10.1002/cite.202200176

Supporting Information available online

Dedicated to Prof. Dr. Christian Wandrey on the occasion of his 80th birthday

Oxidative alkene cleavage is a highly interesting reaction to obtain aldehydes and ketones. The Mn-dependent protein TM1459 from *Thermotoga maritima* can catalyse alkene cleavage of styrene derivatives in the presence of *tert*-butyl hydroperoxide. Despite the high thermal stability of the enzyme, it gets inactivated during the reaction. The data reported here indicate that auto-oxidation is responsible for the low stability of TM1459 in the oxidative environment required for the alkene cleavage reaction. By targeting the exchange of residues prone to oxidation, this phenomenon was successfully prevented. Importantly, the stability to oxidation conveyed by the amino acid exchanges led to increased enzyme activity. However, the exchanges resulted in slightly modified positions of two of the four metal-binding amino acids, thereby strongly impacting metal binding.

Keywords: Alkene cleavage, Amino acid oxidation, Cupin, Stability

Received: September 07, 2022; *revised:* December 18, 2022; *accepted:* January 26, 2023

1 Introduction

Oxidative alkene cleavage is one of the paramount reactions in organic chemistry. The reaction products are aldehydes and ketones, which are applied especially in the flavour and fragrance industry due to their volatility and resulting olfactive property [1], but also in the pharmaceutical industry, where they often serve as precursors for alcohols, amines, cyanohydrins, nitroalcohols, carboxylic acids and esters, or alkanes. There are two main methods to carry out this reaction chemically: 1) dihydroxylation followed by oxidative glycol cleavage and 2) ozonolysis. The major disadvantages of these two methods are the requirement for environmentally unfriendly or toxic compounds for the former method and the low level of safety with ozonolysis [2]. Enzyme-catalysed oxidative alkene cleavage is much safer and works under mild conditions. Several enzymes can perform this reaction including oxygenases and peroxidases, however, in most cases it is a minor side reactivity that leads to low yields [3, 4]. In 2015, we discovered oxidative alkene cleavage activity in TM1459 from *Thermotoga maritima*, an until then uncharacterised protein with known structure [5]. To catalyse the reaction, not only TM1459 but also protein-bound manganese ions and *tert*-butyl hydroperoxide as oxidant are required (Scheme 1). TM1459 cleaves C=C bonds of styrene derivatives and the highest conversion levels were achieved with 4-chloro-α-methylstyrene [5]. As expected for a protein from a hyperthermophilic organism, TM1459 showed high thermal stability. However, while the enzyme is still active at 70 °C, the conversion at higher temperatures was unfavourable as the overall product recovery was low mainly attributed to a loss of substrate and degradation of the hydroperoxide.

[1]Birgit Grill, [1,2]Dr. Tea Pavkov-Keller, [2]Christoph Grininger, [3]Dr. Barbara Darnhofer, [1,2]Prof Karl Gruber, [4]Dr. Mélanie Hall, [1,5]Prof. Helmut Schwab (helmut.schwab@tugraz.at), [1]Dr. Kerstin Steiner (kerstin.steiner11@googlemail.com)

[1]Austrian Centre of Industrial Biotechnology, Petersgasse 14, 8010 Graz, Austria.

[2]University of Graz, Institute of Molecular Biosciences, Humboldtstraße 50, 8010 Graz, Austria.

[3]Medical University of Graz, Core Facility Mass Spectrometry, Stiftingtalstraße 24, 8010 Graz, Austria.

[4]University of Graz, Institute of Chemistry, Heinrichstraße 28, 8010 Graz, Austria.

[5]Graz University of Technology, Institute of Molecular Biotechnology, Petersgasse 14, 8010 Graz, Austria.

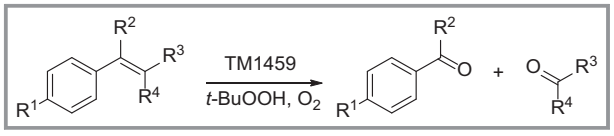

Scheme 1. Oxidative alkene cleavage of styrene derivatives by TM1459.

Fink et al. engineered TM1459 by site-saturation mutagenesis and focussed mostly on the amino acids of the active site: Arg39, Phe41, Ile49, Trp56, Ile60, Phe94, Phe104, Cys106, and Ile108 [6]. Several variants with increased activity were found. Amino acid exchanges at the C-terminus showed higher influence on enzyme activity than others. The best conversion of α-methylstyrene was achieved with the variants at position C106, such as TM1459-C106Q. Despite the high thermal stability of the enzyme, it gets inactivated during the reaction after a few hours. In the current manuscript, it is reported that oxidation of several amino acids is the reason for the protein inactivation. The oxidation of proteins and the covalent modification of amino acids can be caused by many reagents such as reactive oxygen species, ozone [7], metal ions [8], and oxidoreductases [9]. The most commonly modified amino acid residues are cysteine, methionine, tyrosine, tryptophan, histidine, and proline [10]. Consequences of protein oxidation are activity loss of enzymes [9], increased protein aggregation, proteolysis, and altered immunogenicity [11].

Since TM1459 with its general high stability and high expression level in *Escherichia coli* is a highly attractive biocatalyst, which can also perform Michael additions of nitroalkanes and act as peroxygenase depending on the bound metal ion [12, 13], we set out to protect TM1459 against oxidation by exchanging affected amino acids (see Fig. S1 in the Supporting Information). In addition, the general activity of TM1459 was further improved by random mutagenesis.

2 Materials and Methods

2.1 General

All chemicals were purchased from Sigma-Aldrich GmbH (Vienna, Austria) or Carl Roth GmbH (Karlsruhe, Germany) if not stated otherwise. Materials for molecular biology were obtained from Thermo Fisher Scientific (Vienna, Austria) or New England Biolabs (Frankfurt, Germany) if not specifically mentioned. *E. coli* TOP10F' cells were used for plasmid propagation. For expression of pET-based expression vectors, *E. coli* BL21 (DE3) Gold was used. The bacterial strains were obtained from Life Technologies (Carlsbad, CA, USA). All primers were obtained from Integrated DNA Technologies Inc. (Leuven, Belgium). Synthetic genes were ordered from Geneart (Thermo Fisher Scientific). Lysogeny-broth agar plates (LB-Agar (Lennox)) and liquid media, LB-Broth (Lennox) were supplemented with 40 µg mL^{-1} of kanamycin. Plates used for screening were supplemented with 0.1 mM manganese chloride ($MnCl_2$) and optional 0.5 mM isopropyl-beta-D-thiogalactopyranoside (IPTG). DNA concentration was measured on a NanoDrop 2000 spectrophotometer from Thermo Fisher Scientific Inc. The total protein content of cleared lysates was routinely determined with the Bio-Rad protein assay (Bio-Rad, Hercules, CA, USA). For SDS-PAGE, NuPAGE® 4–12 % Bis-Tris gels, 1.0 mm, (Life Technologies) were used with NuPAGE MES SDS running buffer.

2.2 Generation of Variants by Rational Design

Amino acids I2, Y7, M38, W56, and Y83 were targeted by site-directed mutagenesis using primer pairs listed in Tab. S1. The mutations were introduced by overlap-extension PCR using standard PCR conditions and a Phusion HF Polymerase. The plasmid pET26b-TM1459-C106Q [6] was used as template and the purified PCR products were religated into the vector pET26b(+) using *Nde*I and *Hind*III restriction sites. For subsequent double, triple, quadruple, and quintuple variants, site-directed mutagenesis was performed using plasmids as templates, which carried already one or more of the desired mutations. Electrocompetent *E. coli* TOP10F' cells were transformed with the constructs and after regeneration, the cells were plated on LB-Kan agar. After confirmation of the presence of the insert by colony PCR, plasmids were isolated using the GeneJET Plasmid-Miniprep Kit. The correct insertions of the mutations were confirmed by sequencing (Microsynth Austria GmbH, Vienna, Austria). Correct plasmids were used to transform the expression strain *E. coli* BL21 (DE3) Gold.

2.3 Random Library Generation

Random mutagenesis of TM1459-C106Q was performed by error prone PCR. The reaction was performed in a total volume of 50 µL containing 2 ng of template DNA (pET26b-TM1459-C106Q), 0.4 µM of forward and reverse primers each (TM1459_for and TM1459_rev, Tab. S1), 200 µM dATP, dGTP, dCTP, and dTTP (library 1) or 100 µM dGTP and dCTP and 300 µM dATP and dTTP (library 2), 0.1 mM $MnCl_2$, 5 mM $MgCl_2$, 1× reaction buffer and 2.5 U of DreamTaq Polymerase. The PCR product was purified (Wizard SV PCR and Clean-Up System; Promega, Madison, WI, USA) and used as megaprimers for quick change PCR. The reaction was performed in a total volume of 50 µL containing 1 ng of template DNA (pET26b-TM1459), 300 ng of megaprimer, 200 µM dATP, dGTP, dCTP, and dTTP as dNTP mix, 0.2 mM $MnCl_2$, 1× reaction buffer and 2.5 U of Pfu Ultra HF Polymerase (Agilent Technologies, Santa Clara, CA, USA). The PCR products were purified as

mentioned above. For removal of the methylated parent plasmid, the PCR products were digested with *Dpn*I (20 U) for 2 h at 37 °C and subsequent inactivation for 30 min at 70 °C. The desalted libraries were used for the transformation of *E. coli* TOP10F' cells. For each library, three aliquots of electro-competent *E. coli* TOP10F' cells (80 µL) were transformed with 5 µL of desalted mutagenised pET26b-TM1459-C106Q plasmids. The three transformations were combined and regenerated in LB medium. After 1 h of regeneration at 37 °C, kanamycin was added before another hour at the same conditions. 1 mL of the cell suspension was used to inoculate a 10 mL LB-Kan pre-culture. The pre-culture was incubated overnight at 37 °C and 120 rpm. The pre-culture was centrifuged for 5 min at 2970*g* and used for plasmid isolation using GeneJET Plasmid Miniprep Kit resulting in a mixed plasmid library. Ten arbitrary clones of the transformation plates were chosen, their plasmids isolated and sent for sequencing to Microsynth AG (Vienna, Austria). Based on these sequencing results, the mutation rate was determined.

2.4 Library Screening

Electro-competent *E. coli* BL21 Gold (DE3) cells were transformed with the libraries. The transformants were grown on large square LB-Kan agar plates overnight at 37 °C. The colonies were transferred to 384-well plates (Nunc, Thermo Scientific Vienna, Austria) filled with 55 µL LB-Kan medium with a QPix picking robot (Genetix, now Molecular Devices LLC Munich, Germany). Some wells were left empty for controls. The 384-well microtiter plates were incubated overnight at 37 °C. The next day, 35 µL of sterile 30 % glycerol were added to each well and the plates were sealed before storage at –80 °C. The libraries were expressed in deep well plate cultivation. The deep well plates containing 750 µL LB-Kan medium per well were inoculated by transferring the library with a 96-well replicator from the 384-well microtiter plates. For the controls as above, single colonies of agar plates were used for inoculation with sterile toothpicks. Incubation was done overnight using an orbital shaker at 320 rpm in a 37 °C incubation room. For the main culture, 750 µL LB-Kan medium per well supplemented with 100 µM $MnCl_2$ were inoculated with 25 µL of the overnight culture. Incubation was done using an orbital shaker at 320 rpm in a 37 °C incubation room. After 6 h, protein expression was induced using 50 µL LB-Kan medium supplemented with 100 µM $MnCl_2$ and 1.65 mM IPTG. Incubation was done for another 17 h at 25 °C and the cells were harvested the next day by centrifugation for 15 min at 2970*g*. The supernatant was discarded and the pellets were frozen at –20 °C. For cell lysis, 300 µL of lysis buffer (0.28 mg mL^{-1} lysozyme from chicken egg white (~70 000 U mg^{-1}), 4 U mL^{-1} Benzonase Nuclease (purity > 90 %, 250 U µL^{-1}, Merck KGaA Vienna, Austria), 0.2 % Triton X-100 in 50 mM NaPi, pH 8) were pipetted onto the frozen pellets and the deep well plate was vortexed until the pellets were completely resuspended. The plates were shaken at 1000 rpm at room temperature for 1 h followed by centrifugation for 15 min at 2970*g* and 4 °C. The cell-free lysate was then directly used for high-throughput screening assay.

The high-throughput screening assay for oxidative alkene cleavage activity was performed as described before [6]. 130 µL of protein solution (either cell-free lysate or 2 mg mL^{-1} purified protein) were mixed with 50 µL of substrate mix (46 % ethanol, 36 mM α-methylstyrene (final concentration in reaction 10 mM), 90 mM *tert*-butyl hydroperoxide (final concentration in reaction 25 mM), and 0.2 % Triton X-100 in 50 mM NaPi, pH 8 buffer) in 96-well microtiter plates. The plate was sealed with adhesive film and incubated for 2 h at 37 °C. 50 µL of detection mix (10 % ethanol, 3.5 % (w/v) vanillin, 2 M NaOH) were added per well. The plate was sealed again and incubated for another 30 min at 37 °C. The absorption was measured at 442 nm using an EON Microplate Spectrophotometer. The absorbance value of the blank (lysate without expressed TM1459) was subtracted from all other absorbance values. The absorbance values were then normalised to the parent clone and the activity of α-methylstyrene conversion for random clones was given as percent compared to the parent.

2.5 Protein Production and Purification

E. coli BL21-Gold (DE3) cells harbouring pET26a-TM1459 variants were grown in 10 mL LB-Kan (40 µg mL^{-1}) medium at 37 °C overnight. Subsequently, 400 mL LB-Kan medium supplemented with 100 µM $MnCl_2$ in 1 L shake flasks were inoculated with the preculture and incubated at 37 °C at 120 rpm. Gene expression was induced at OD600 of 0.8 by adding IPTG to a final concentration of 0.1 mM and the temperature was reduced to 25 °C for 20 h. The cells were harvested by centrifugation for 15 min at 4 °C and 5000*g* and stored at –20 °C until further use. Cells were resuspended in 50 mM sodium phosphate buffer (NaPi), pH 8 and disrupted by sonication (Branson Sonifier S-250; 6 min, 80 % duty cycle, 70 % output). The cell lysate was centrifuged for 1 h at 48 250*g*. The cell-free lysate was filtered through 0.45 mm syringe filters. If needed, the samples were concentrated (using Vivaspin 20 Centrifugal Filter Units 10 000 Da molecular-weight cut-off; Sartorius Goettingen, Germany) and frozen until further use.

For heat purification, cell-free lysates were incubated with 4 U mL^{-1} benzonase for 1 h at 37 °C and 300 rpm in a thermomixer device to remove DNA and, subsequently, for 10 min at 75 °C and 900 rpm to precipitate *E. coli* proteins. Afterwards, denatured proteins were removed by centrifugation for 10 min at 16 300*g* and 4 °C. The supernatant was filtered through syringe filters with a pore size of 0.45 µm. Buffer exchange was done using PD-10 desalting columns.

Alternatively, a two-step chromatography purification was performed by ion exchange chromatography on a

HiTrap™ Q FF (50 mM BisTris containing 30 mM NaCl (buffer A) and 1 M NaCl (buffer B), pH 6.5, gradient 12–100 % buffer B) followed by size-exclusion chromatography in Tris-buffered saline, pH 7.9 on a HiLoad™ 16/600 Superdex™ 75 (GE Healthcare Braunschweig, Germany).

If manganese was reconstituted into purified proteins, 540 µL of 2.2 mg mL^{-1} protein solution was incubated for 2 h at room temperature with 60 µL of 3 mM $MnCl_2$. After this period, the protein was directly used for the assay or the unbound manganese ions were removed with PD-10 desalting columns.

The protein concentration was determined with a NanoDrop 2000c spectrophotometer.

2.6 Protein Oxidation Assay

To 1 mL of heat-purified protein (TM1459 and its variants or a transaminase as control, 1.5 mg mL^{-1}) in 50 mM sodium phosphate buffer, pH 7, *t*-BuOOH was added to a final concentration of 30 mM. Optionally, also 100 µM manganese was supplemented either as Mn^{2+} as manganese chloride dissolved in water or as Mn^{3+} as manganese acetate dissolved in ethanol. Samples were taken at different time points. The reaction was stopped with an equimolar amount of sodium disulfate. The samples were analysed via SDS-PAGE analysis as oxidised proteins are visible as smeared bands on the gel.

2.7 Mass Spectrometry

Purified TM1459 and its variants (pre-incubated with Mn for reconstitution) were diluted to a concentration of 4 mg mL^{-1} with 50 mM sodium phosphate buffer, pH 7. 100 µL of each variant were placed on ice as control, whereas 100 µL were incubated with 30 mM *t*-BuOOH at 37 °C and 400 rpm for 4 h. The oxidation reaction was stopped by addition of 100 µL of 30 mM sodium disulfite. The buffer was exchanged to a 50 mM ammonium bicarbonate buffer with PD-10 desalting columns. The proteins were concentrated using Vivaspin 20 columns to a concentration of about 1 mg mL^{-1}.

10 µg protein were digested by adding 0.2 µg of Promega-modified trypsin and shaking overnight at 550 rpm at 37 °C. 100 µg of digested proteins were acidified up to 0.1 % formic acid, 5 % acetonitrile and separated by nano-HPLC (Dionex Ultimate 3000) equipped with a C18, 5 µm, 100 Å, 5×0.3 mm enrichment column and an Acclaim PepMap RSLC nanocolumn (C18, 2 µm, 100 Å, 500×0.075 mm) (all Thermo Fisher Scientific, Vienna, Austria). Samples were concentrated on an enrichment column for 2 min at a flow rate of 5 µL min^{-1} with 0.5 % trifluoroacetic acid as isocratic solvent. Separation was carried out on the nanocolumn at a flow rate of 250 nL min^{-1} at 60 °C using the following gradient, where solvent A is 0.1 % formic acid in water and solvent B is acetonitrile containing 0.1 % formic acid: 0–2 min: 4 % B; 2–90 min: 4–25 % B; 90–95 min: 25–95 % B, 96–110 min: 95 % B; 110–110.1 min: 4 % B; 110.1–125 min: 4 % B. The sample was ionised in the nanospray source equipped with stainless steel emitters (ES528, Thermo Fisher Scientific, Vienna, Austria) and analysed in an Orbitrap Velos Pro Mass Spectrometer (Thermo Fisher Scientific, Waltham, MA, USA) operated in positive ion mode, applying alternating full scan MS (m/z 400 to 2000) in the ion cyclotron and MS/MS by CID of the ten most intense peaks with dynamic exclusion enabled. The LC-MS/MS data were analysed by searching a database containing all proteins of interest and common contaminants with Mascot 2.4.1 (MatrixScience, London, UK) and Proteome Discoverer 1.4. Detailed search criteria: enzyme, Trypsin; maximum missed cleavage sites, 2; N-terminus, hydrogen; C-terminus, free acid; variable oxidation on methionine, cysteine, tyrosine, histidine, and tryptophan; search mode, homology search; maximum precursor charge, 3; precursor mass tolerance, 10 ppm; product mass tolerance, ±0.7 Da.; 1 % false discovery rate. Data was filtered according to stringent peptide acceptance criteria, including mass deviations of ±10 ppm, minimum 2 peptides per protein, Mascot ion score of at least 17 and a position rank 1 in Mascot search.

2.8 Thermal Shift Assay

The proteins were diluted to a concentration of 2 mg mL^{-1} with 50 mM sodium phosphate buffer, pH 7. 20 µL of a mastermix composed of reaction buffer and SYPRO® Orange dye (Sigma-Aldrich Darmstadt, Germany, final dilution in reaction 1:5000) were filled into 96-well optical reaction plates (Invitrogen Vienna, Austria) and 5 µL of protein (10 µg final amount) were added. The increase of the fluorescence of the SYPRO Orange probe during the unfolding of the protein (temperature increased 1 °C per min from 20 to 95 °C) was measured in an Applied Biosystems 7500 Fast Real-Time PCR System (Life Technologies Vienna, Austria) with excitation at 490 nm and emission at 575 nm. Measurements were performed in duplicate or triplicate.

2.9 CD Spectroscopy

Protein samples were diluted to about 0.5–0.8 mg mL^{-1} protein in 50 mM sodium phosphate buffer, pH 7. CD spectroscopy was done using a J-715 spectropolarimeter. Settings: 185–260 nm, continuous, 1 s for one data point, 1.0 nm distance between data points, triplicate. Temperature scans were performed with the following settings: 25–95 °C, 195–260 nm, 1 °C min^{-1} heating, temperature course for 215 nm (specific for beta-sheets).

2.10 Luminol Assay

This assay detects metals in small amounts using luminol and 4-(2-pyridylazo)resorcinol (PAR) [14]. The protein samples were diluted to 10 mg mL^{-1} or lower. The assay was conducted in black 96-well microtiter plates and fluorescence measurements were done with a Synergy™ Mx Microplate Reader. A standard curve was made using defined amounts of $MnCl_2$ in ddH_2O. The final amount in the wells was 1, 0.5, 0.2, 0.1, 0.05, and 0.01 nmol $MnCl_2$. Each standard contained 10 µg BSA. The blank also contained 10 µg of BSA. 40 µL of 8 M urea were pipetted into each well. 10 µL of the standard/blank/sample were added. 100 µL of luminol (11 mM dissolved in 0.5 M Na_2CO_3 containing 0.7 % H_2O_2) were added, the mix was incubated for 3 min before luminescence was measured for 10 ms. Afterwards, 10 µL of PAR (2 mM dissolved in 96 % EtOH) were added and again incubated for 3 min before the luminescence was again measured for 10 ms. Then, the microtiter plate was incubated for 2 h at room temperature and centrifuged for 2 min at 2970*g* before the absorption at 492 nm was measured in an EON microplate spectrophotometer. With the calibration curve, the protein concentration, and the dilution factor, the percentage of molar amount of manganese per molar amount of protein could be calculated. In the first measurement, the metals iron, copper, and cobalt gave a positive signal. In the second measurement, the metals iron, manganese, and cobalt were detected, and in the third measurement, the metals copper, cobalt, nickel, and zinc were monitored.

2.11 ICP-OES Analysis

Metals analysis was performed by axially viewed ICP-OES (Spectro Ciros Vision EOP, Spectro Analytical Instruments, Kleve, Germany). Protein samples (500 µL of 5–10 mg mL^{-1} purified protein solutions in 50 mM KPi, pH 6.0) were digested with 1 mL HCl, 2 mL HNO_3, and 2 mL H_2O using a pressurised microwave digestion system (Multiwave 3000, Anton Paar, Graz, Austria). The microwave power was ramped up to 1400 W over a period of 10 min. After a further 20 min of continued heating at 220 °C, the content of the vessels was cooled and diluted to a final volume of 20 mL. Scandium was added to the solutions as an internal standard. ICP-OES calibration solutions (0.04–10 mg L^{-1}) were prepared from a 100 mg L^{-1} multi-element stock (28-element ICP standard solution, Carl Roth Karlsruhe, Germany) in 3 vol % HNO_3. The concentrations of Mg, Cu, Fe, Mn, and Zn were determined under robust plasma conditions by ICP-OES [15]. The ICP was operated at 1350 W RF power, 12.5 L min^{-1} cooling gas flow, 0.6 L min^{-1} auxiliary gas flow, and 0.83 L min^{-1} nebulizer gas flow. A standard torch with a 2.5 mm ID injector and a cross-flow nebulizer with a Scott-type spray chamber were used. The following emission lines were used: Cu, 324.754 nm; Fe, 259.941 nm; Mn, 257.611 nm; Sc, 361.384 nm; Zn, 213.856 nm. Metal loading was calculated based on the molar protein concentrations and the measured molar concentrations of the metals.

2.12 Protein Crystallisation

TM1459 variants were purified by two-step protein chromatography. Prior to crystallisation 1 mM $MnCl_2$ was added to the protein solution. Crystallisation trials were set up at 16 °C by the sitting-drop vapour diffusion method using the Oryx8 Protein Crystallisation Robot (Douglas Instruments Birkshire, UK) and commercial crystal screens: Index (Hampton Research Loughborough, UK), JCSG+, Morpheus I and Midas (Molecular Dimensions Rotherham, UK). The drop volume was 1 µL with a 1:1 ratio of protein to reservoir solution. Initial protein concentrations used for crystallisation trials were 14.2 mg mL^{-1} for variant 208, 8 mg mL^{-1} for AIFQ, and 16 mg mL^{-1} for C106Q.

Crystals appeared after a few days under the following conditions: JCSG+ B11 for 208 (1.6 M sodium citrate tribasic dihydrate pH 6.5), Index A6 for AIFQ (0.1 M Tris pH 8.5, 2.0 M ammonium sulfate), and JCSG+ C2 for C106Q (1 M LiCl, 0.1 M citrate pH 4.0, 20 % PEG6000). X-ray diffraction datasets were collected from several crystals at the synchrotron beamlines XRD1 (Elettra, Trieste, Italy), P11 (PETRAIII, DESY, Hamburg, Germany), and P14 (PETRAIII, EMBL, Hamburg, Germany). The data were processed using the program XDS [16]. Structures were solved by molecular replacement using Phaser [17] and the structure of the wild-type TM1459 (PDB code 1VJ2; [18]) as the search template. The model was refined with the PHENIX package [19, 20]. Data collection and refinement parameters for the best data sets are summarised in Tab. S2. Coordinates and structure factors have been deposited in Protein Data Bank under the accession numbers 8AWN, 8AWO, and 8AWP.

2.13 Biotransformations

The conversion in an aqueous reaction system was done on a 500 µL scale in microcentrifuge tubes. The reaction mixture contained 20 mM substrate (4-chloro-α-methylstyrene or α-methylstyrene), 60 mM *t*-BuOOH and 1 mg mL^{-1} enzyme (heat-purified TM1459 variants, ~77 µM) in 50 mM sodium phosphate buffer, pH 7. The substrate was added from a 1 M stock solution in ethanol. The reaction was started by the addition of enzyme and incubated overnight at 30 °C and 140 rpm in a multitron shaking incubator. All reactions were performed as duplicates. Standard curves for the substrates (4-chloro-α-methylstyrene and α-methylstyrene) as well as for the products (4-chloroacetophenone and acetophenone) were established using five different concentrations from 1–20 mM. The conversion in a

biphasic reaction system was done on a 500 µL scale in microcentrifuge tubes. The reaction mixture contained 50 mM substrate (4-chloro-α-methylstyrene), 150 mM *t*-BuOOH and 1 mg mL^{-1} enzyme (heat-purified and Mn-preincubated TM1459 variants) in 50 mM sodium phosphate buffer, pH 7, with 5 vol % ethyl acetate. The reaction was started by the addition of enzyme and incubated overnight at 30 °C and 140 rpm in a shaking incubator. Standard curves were established for 4-chloroacetophenone using five different concentrations from 2.5–50 mM in duplicates. The reactions were extracted two times with ethyl acetate spiked with 20 mM 1-decanol as internal standard. The combined organic phases were dried over anhydrous Na_2SO_4. GC analysis was performed on an Agilent 7890B GC system equipped with a flame ionisation detector and the column HP-5 19091J-413 (30 m, 0.32 mm ID, 0.25 µm film, J&W Scientific, Agilent Technologies Vienna, Austria). The temperature program is given in Tab. S3. The GC-MS analysis was carried out on a 7890A GC System (Agilent Technologies Vienna, Austria), equipped with a 5975C inert XL MSD mass spectrometer (Agilent Technologies Vienna, Austria) and an HP-5MS column (30 m, 0.25 mm ID, 0.25 µm film, J&W Scientific, Agilent Technologies Vienna, Austria). For the temperature program, see Tab. S4.

3 Results and Discussion

TM1459 from *Thermotoga maritima*, which belongs to the cupin superfamily of proteins, catalyses oxidative alkene cleavage. During our previous work it was observed that, while the enzyme is extremely heat stable and can be purified by heating the sample to 75 °C, the enzyme was inactivated over time in the biotransformations containing substrate, phosphate buffer, and *tert*-butyl hydroperoxide. Thus, this observation was further investigated. Samples were taken at different time points of the reaction. SDS-PAGE analysis showed that the original protein band disappeared over time, while a smear of higher molecular mass appeared (data not shown), indicating some modification of the protein. Peptide fingerprinting by mass spectrometry revealed that several amino acids (M1, Y7, M38, Y83, H52, H54, H58, H92, and C106) were oxidised during the reaction, which corresponded well with literature reports of oxidizable amino acids [10].

To test whether the enzyme was responsible for the oxidation of the amino acids (i.e., auto-oxidation) or if the amino acids were oxidised by the presence of manganese and *t*-BuOOH alone, a transaminase was incubated with and without TM1459-C106Q, but always in the presence of *t*-BuOOH and Mn either as Mn^{2+} or Mn^{3+}. Although Mn^{3+} promoted aggregation of the transaminase, the typical smear of the oxidised enzyme and the disappearance of the original band were only observed in the presence of TM1459-C106Q (Fig. S2), indicating that the oxidation was indeed mediated by this protein.

3.1 Increasing the Stability of TM1459 against Oxidation

To stabilise the enzyme against auto-oxidation, the oxidised amino acids were exchanged by site-directed mutagenesis and screened for activity in a microtiter plate assay. In this assay, α-methylstyrene is converted to acetophenone by TM1459 variants in the presence of *t*-BuOOH. The detection of the product is done by addition of vanillin, which undergoes an aldol condensation reaction with acetophenone under basic conditions, leading to the formation of a yellow-coloured condensation product [21]. Furthermore, the oxidation stability was tested by incubating the most active variants with hydroperoxide and subsequent analysis on SDS-PAGE gels. Metal loading and thermal stability were also investigated for the best variants.

Four histidine residues are responsible for the metal binding, and during characterisation of TM1459, it was shown that amino acid exchanges to Ala, Glu, or Gln at positions H52, H54, and H92, respectively, resulted in an almost complete loss of Mn binding and activity, and at position H58 significantly reduced Mn binding and activity (unpublished data). Thus, these amino acids cannot be exchanged. The positive effect of the exchange of C106 has been reported before [6]. Therefore, variant TM1459-C106Q together with the wild-type protein were used as parent for subsequent protein engineering to exchange Y7, M38, and Y83. These amino acids were exchanged one by one and by combining as many exchanges as possible resulting in single, double, triple, and finally quadruple variants. The variants were tested for their activity and oxidation stability (Tab. S5, Fig. S3) and the two most active and stable variants (Y7A/M38I/Y83F/C106Q, short TM1459-AIFQ, and Y7F/M38I/Y83F/C106Q, short TM1459-FIFQ) were used as templates to exchange I2 to smaller amino acids (alanine and glycine) variants to promote the cleavage of the starting methionine during translation [22]. The variants were again characterised regarding their activity and oxidation stability. Like the wild-type enzyme and the parent variants all of the new variants were well expressed as soluble proteins in *E. coli* (Fig. S4). In the case of I2 variants, the cleavage of the starting methionine was confirmed by mass spectrometry. Unfortunately, the quintuple variants of TM1459-I2AorG/Y7AorF/M38I/Y83F/C106Q were not more stable against oxidation than their quadruple parents (data not shown). They were also less active in the standard screening assay with α-methylstyrene, especially if they were heat-purified, where the activity is significantly reduced, which is in contrast to the parent quadruple variants, which were more active when they were heat-purified (Fig. S5). The manganese content in heat-purified TM1459 variants was investigated with the highly sensitive luminol assay. The wild type showed the highest manganese loading and the more amino acid exchanges a variant had, the less manganese was bound as depicted in Tab. 1. Although the exchanged amino acid residues were not part of the metal binding site, they

seemed to negatively influence the metal binding ability (this was later confirmed by ICP-OES for some variants, see below). While the wild-type protein has constantly shown to have a metal loading of 40 % and more after heat purification (up to 70 % in other samples), the quadruple variants were in the range of 16 % and the quintuple variants of only 9 %. The thermal stability of the variants was measured by a Thermofluor assay. Both TM1459-WT and TM1459-C106Q did not denature in the assay, indicating stability above 95 °C. The quadruple variants were slightly less stable and the quintuple variants were the least stable, displaying still a high melting point T_m of 78 °C. Thus, during heat purification at 75 °C, the quintuple variants were likely partially denatured and inactivated.

Table 1. Manganese loading (luminol assay) and melting point (Thermofluor assay) of heat-purified TM1459 variants. The relative molarity of manganese per protein is given. Samples were measured in triplicate.

Variant	Manganese content [mol %]	Melting point [°C]
WT	40.6	–[a)]
C106Q	26.9	–[a)]
AIFQ	16.8	88
FIFQ	16.0	89
AAIFQ	8.4	78
GAIFQ	8.7	78
AFIFQ	8.6	84
GFIFQ	9.3	78

[a)] Protein did not denature during measurement (20–95 °C).

Thus, it was subsequently tested if the variants were more active if they were purified by classical protein chromatography. Surprisingly, these enzymes were even less active (Fig. S6). Again, it was confirmed by luminol assay that the metal loading of the variants was significantly lower than that of the wild type (in this case also TM1459-C106Q contained only 16 % Mn, while the loading of the wild type was higher at about 70 %). The thermal stability established by a Thermofluor assay was the same as for heat-purified enzymes (data not shown). Although manganese was added during shake flask cultivation, it did not seem to bind tightly to the variants and the metal was lost most probably during protein purification.

After pre-incubation of the TM1459 variants with manganese, they regained their oxidative cleavage activity on α-methylstyrene as shown in Fig. 1, with a level of activity exceeding that of the wild type.

To further understand whetther metal binding alone was responsible for the lower activity of the quintuple variant, measurements by CD spectroscopy were performed. The wild-type enzyme and the variants C106Q, AIFQ, and

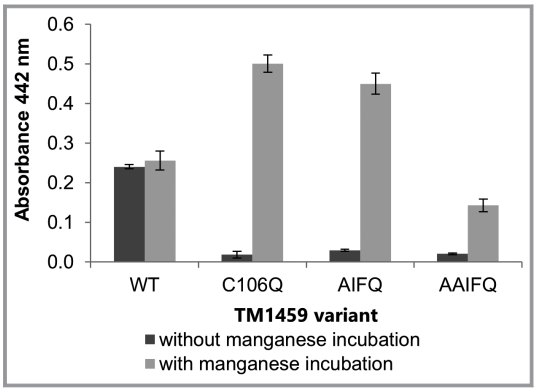

Figure 1. Microtiter plate assay. Conversion of 10 mM α-methylstyrene by TM1459 and its variants purified by protein chromatography with and without manganese pre-incubation and monitored by the vanillin assay at 442 nm.

AAIFQ were analysed using both purification methods. The standard spectra of different TM1459 variants looked highly similar as depicted in Fig. S7 except for variant TM1459-AAIFQ, which did not show such a distinct bow at 220 nm as the other variants. This effect was observed for both purification methods. In addition, temperature curves were recorded with the variants purified by protein chromatography (Fig. S8). As already observed in the Thermofluor assay, TM1459 variants were highly temperature-stable and began to unfold at about 70 °C at the earliest. None of the variants was completely unfolded at 95 °C. Downscans were also performed for some variants (Fig. S9). It can be seen that the variants refolded when the temperature decreased. The spectrum of refolded TM1459-C106Q was more similar to its original state than the refolded spectrum of variant TM1459-AAIFQ.

Purified and manganese pre-incubated TM1459 variants were incubated with *t*-BuOOH and analysed by mass spectrometry (Tab. 2) to monitor the oxidation of amino acids.

Table 2. MS analysis of oxidised amino acid residues of TM1459 variants.

TM1459 variant	Oxidised amino acid
WT	M1, Y7, M38, W56, H58, Y83, H92
C106Q	M1, Y7, M38, H52, H54, W56, H58, Y83
AQ	M1, M38, H52, H54, W56, Y83, H92
AIFQ	M1, H54, W56, H92
AAIFQ	H52, H54, W56, H92

In addition to the replaced amino acids, the histidine residues building up the metal binding site and also Trp56 were oxidised. Trp56 had not been observed to be oxidised before and was therefore not exchanged in the first round of mutagenesis. The TM1459 variants with Trp56 exchanged to Ala

and Glu were subsequently generated based on the best quadruple and quintuple variants (TM1459-AIFQ and TM1459-AAIFQ). While the W56A exchange did not increase the activity, the variants with W56D (TM1459-AIDFQ and TM1459-AAIDFQ) showed significantly higher conversions than their precursors in the standard screening assay (Fig. 2).

The activity of TM1459-AIDFQ (Y7A/M38I/W56D/Y83F/C106Q) was about twice as high as variant TM1459-C106Q and showed the highest product formation from all variants in the spectrophotometric assay. The amino acid residue Trp56 might have a beneficial influence on the activity of TM1459 for two reasons. Firstly, tryptophan was exchanged to an amino acid residue that cannot be oxidised. This was confirmed by the oxidation assay (Fig. S10). Even after overnight incubation with *t*-BuOOH, 82 % of variant TM1459-AIDFQ were left in non-oxidised form compared to its precursor TM1459-AIFQ (46 %). Secondly, Trp56 is located in the cavity of TM1459 near the metal binding site and might therefore play a role in substrate binding and/or access to the binding site. In earlier site saturation mutagenesis studies, Trp56 had already been a target and the single variant W56D had shown about 150 % activity compared to the wild-type enzyme [6].

3.2 Improving the Activity by Random Mutagenesis

Subsequently, attempts to improve the activity of TM1459 by random mutagenesis were initiated. Considering that TM1459-C106Q showed the highest metal loading among the variants, it was chosen as parent for random mutagenesis. The most active variants should later be combined. The library generation was done using megaprimers, which covered the whole TM1459 gene. The megaprimers were synthesised by error-prone PCR applying various $MnCl_2$ concentrations and imbalanced dNTP concentrations to create different mutation rates. In total, 10 300 variants of the two most suitable libraries with 1.44 (library 1) and 3.22 (library 2) mutations per gene were finally again screened in a microtiter plate assay using cell-free lysate for the conversion of α-methylstyrene. 8 % of the variants were more active than the parent TM1459-C106Q (Tab. 3).

Table 3. Relative activity of the variants compared to parent TM1459-C106Q.

Category	Library 1 [%]	Library 2 [%]
Mutation rate/gene	1.44	3.22
"Parent" (90–110 %)	22	25
"Hits" (> 110 %)	8	5
50–90 % activity	30	27
10–50 % activity	11	10
Inactive (< 10 %)	29	33

The 22 best clones of each library were re-screened in quadruplicate and their plasmids were isolated and sent for sequencing (Tab. S7). Many amino acid exchanges were found more than once. The amino acid exchange F104L was found seven times. This amino acid exchange was also found in previous work [6] to increase the activity towards α-methylstyrene of the wild type. Nevertheless, this amino acid exchange had not been investigated yet in combination with C106Q. The amino acid residues K18, M38, R39, E50, I60, and C106 were also exchanged multiple times. The amino acid exchange C106L appeared three times. Fink et al. [6] had already shown that this variant was slightly better than TM1459-C106Q in terms of conversion of α-methylstyrene, but TM1459-C106Q was significantly better when converting other substrates such as indole and tryptophan. Noteworthy, M38 was one of the targets in the rational mutagenesis for increased oxidative stability. While some of these amino acids mentioned before were always replaced by the same amino acid (M38I, I60F), others were replaced by different ones. E50 was either replaced by valine or glutamic acid. K18 was either exchanged by asparagine or isoleucine and R39 by cysteine or histidine. Interestingly, the variant TM1459-V37M/F104L/C106Q was found twice, once in each library. Compared to TM1459-F104L/C106Q, the triple variant showed almost the same activity, so the effect of V37M is questionable. For a better understanding, the variant TM1459-V37M/C106Q would have to be generated and investigated. The 14 best hits were further characterised. All of them were well expressed and could be heat-purified (Fig. S11). The screening assay for acetophenone formation was performed with purified enzyme with and without manganese

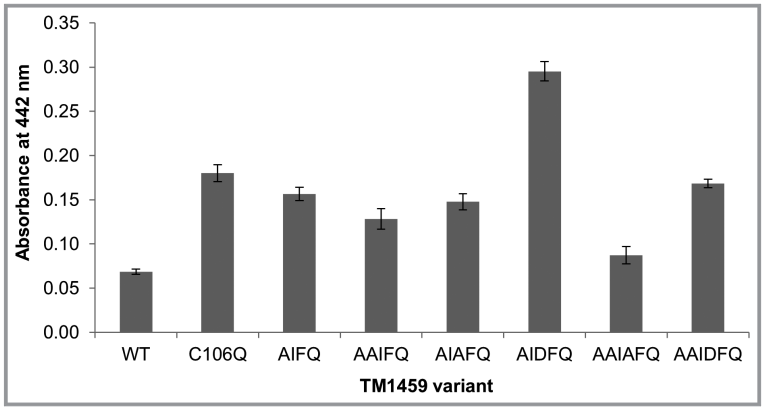

Figure 2. Microtiter plate assay. Conversion of 10 mM α-methylstyrene by TM1459 variants with exchanged tryptophan monitored by the vanillin assay at 442 nm. Each variant was run in octuplicate.

pre-incubation. Without manganese pre-incubation only variant TM1459-208 (V19I/R23H/M38I/I60F/C106Q and three silent mutations) was significantly more active than TM1459-C106Q (data not shown). With manganese pre-incubation variant TM1459-208 also showed the highest product formation with a nearly threefold increase in activity compared to its precursor TM1459-C106Q (Fig. 3). All other hits also showed higher product formation than TM1459-C106Q except for variant TM1459-213. The best variant TM1459-208 did not show higher oxidation stability (Fig. S10), which was not surprising as most of the oxidizable amino acids are still present.

3.3 Biotransformations

4-Chloro-α-methylstyrene was identified as the substrate with the highest conversion by TM1459 [5]. Thus, all promising TM1459 variants of the random engineering were initially tested for overnight conversion of 4-chloro-α-methylstyrene in an aqueous system (data not shown). Since variant TM1459-208 (V19I/R23H/M38I/I60F/C106Q) again achieved the highest conversion of 20 mM 4-chloro-α-methylstyrene, it was combined with the most stable stability variant TM1459-AIDFQ (Y7A/M38I/W56D/Y83F/C106Q) resulting in variant TM1459-Y7A/V19I/R23H/M38I/W56D/I60F/Y83F/C106Q, named combi. Since it was shown that metal loading varies a lot in different enzyme preparations (see above), the metal content of purified and Mn-incubated proteins samples was analysed (Tab. 4). The variants TM1459-208 and TM1459-combi showed a clearly lower Mn-loading and this was also reflected in the conversion data (Fig. S12). However, taking into consideration the proportion of functionally active protein in each sample (i.e., fraction of protein with Mn-loaded active site), the variants TM1459-208 and TM1459-combi displayed much higher enzyme activity, which translated into higher total turnover numbers (TTN), indicating that these variants were overall better performing than TM1459-C106Q. At the lowest enzyme loading (0.1 mg mL^{-1}, ~7.7 µM enzyme), highest TTNs were obtained for all proteins, reaching 8860 for TM1459-208 and 7981 for TM1459-combi, respectively, more than a threefold increase compared to TM1459-C106Q (TTN of 2499) (Tab. 5).

Table 4. ICP-OES analysis. Metal loading was calculated based on the molar protein concentrations and the measured molar concentrations of the metals. No Cu, Fe, and Mg were detected.

TM1459 variant	Mn [%]	Zn [%]
C106Q	47.4	5.7
208	16.7	5.3
AIDFQ	64.8	6.3
Combi	20.4	10.3

Finally, lower peroxide concentrations correlated in general with lower conversion levels, regardless of the variant used (Tab. 5) and the highest product amounts with each variant were obtained at 60 mM peroxide and 1 mg mL^{-1} protein (up to 15 mM product and 75 % conversion with TM1459-C106Q).

4 Structural Characterisation of TM1459-C106Q, TM1459-208, and TM1459-AIFQ

To better understand the influence of the amino acid exchanges on the enzyme structure, the crystal structures of TM1459-C106Q, TM1459-208 (V19I/R23H/M38I/I60F/C106Q), and TM1459-AIFQ (Y7A/M38I/Y83F/C106Q) were determined. In all obtained structures, despite the addition of manganese, no strong electron density was present at the expected manganese position. In TM1459-C106Q and AIFQ variants, an electron density is present in the vicinity of H52 and H54 (Fig. S13), that could be interpreted either as a water molecule or a manganese ion with occupancy lower than 40 % and disintegrated metal coordination.

This is further corroborated by altered conformations of the active site histidines 54 and 58, which are involved in manganese coordination (Fig. 4). Due to the exchange of C106 to Gln (present in all three variants), H58 is pushed towards H54, which is subsequently forced to flip out compared to the original position observed in the wild type [17]. The same is observed for the conformation of R39. These observations can be transferred to all other variants having C106Q amino acid exchange and lower manganese binding capacity.

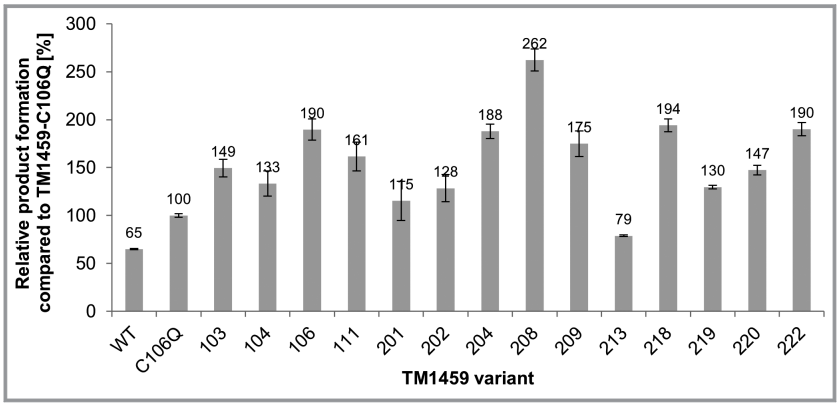

Figure 3. Microtiter plate assay. Conversion of α-methylstyrene by heat-purified TM1459 variants of random engineering (with manganese pre-incubation) and monitored by the vanillin assay at 442 nm. Samples were run in quadruplicate.

Table 5. Total turnover numbers (TTN)[a] obtained in the conversion of 4-Cl-α-methylstyrene by the TM1459 variants under varying reaction conditions.

Variant	Standard[b]	0.1 mg mL^{-1} enzyme[b]	40 mM *t*-BuOOH[c]	20 mM *t*-BuOOH[c]	10 mM *t*-BuOOH[c]
C106Q	413	2498	352	268	315
208	1034	8890	783	568	593
AIDFG	288	1902	240	213	193
Combi	758	7975	579	520	483

[a] TTN (mole of product per mole of active enzyme) was obtained by measuring the amount of formed 4-Cl-acetophenone by GC analysis using a calibration curve with an authentic reference and correlating this amount to the amount of metal-loaded active site (see Tab. 4). For example, 1 mg mL^{-1} (~77 μM) C106Q represents 36.5 μM of functionally active enzyme (47.4 % Mn). [b] Reaction conditions: 1 mg mL^{-1} enzyme (~77 μM), 20 mM 4-Cl-α-methylstyrene and 60 mM peroxide in sodium phosphate buffer (50 mM, pH 7). Incubation was done at 30 °C and 120 rpm overnight. [c] Reaction conditions: same as in b) except for one varying parameter, as indicated.

Three of the amino exchanges (V19I, R23H, and M38I) of variant TM1459-208 are not located in the active site. However, position I60 is located in the active site and, thus, an amino acid exchange to Phe might have an influence on substrate binding (Fig. S14).

5 Conclusion

Taken together, the data indicate that auto-oxidation is responsible for the low stability of TM1459 in the oxidative environment required for the cleavage of styrene derivatives. By targeting the exchange of residues prone to oxidation, this phenomenon was successfully prevented. Importantly, the stability to oxidation conveyed by the amino acid exchanges led to increased enzyme activity, as demonstrated by much higher total turnover numbers for two of the variants. However, metal analysis and subsequent analysis of the protein structures of some variants also showed that the amino acid exchanges, mostly C106Q, resulted in slightly modified positions of two of the four metal-binding amino acids, thereby strongly impacting metal binding. Mn was found to bind less tightly in the variants, and pre-incubation with the metal did not contribute to restoring high levels of bound metal. To translate the higher enzyme activity obtained with two of the variants into high conversion levels, further efforts should be directed at improving the metal binding and increasing the proportion of functionally active enzyme while retaining the engineered stability against auto-oxidation. This engineering campaign demonstrates that TM1459 can be tailored for better stability and activity.

Supporting Information

Supporting Information for this article can be found under DOI: https://doi.org/10.1002/cite.202200176.

We thank Sarah Schmid for excellent technical assistance and Helmar Wiltsche for ICP-OES analysis. This work has been supported by the Federal Ministry of Science, Research and Economy (BMWFW), the Federal Ministry of Traffic, Innovation and Technology (bmvit), the Styrian Business Promotion Agency SFG, the Standortagentur Tirol, the Government of Lower Austria, and ZIT – Technology Agency of the City of Vienna through the COMET-Funding Program managed by the Austrian Research Promotion Agency FFG (grant number FFG 848951). We acknowledge Elettra (Trieste Italy; XRD1 beamline), EMBL (PETRAIII, Hamburg, Germany; P14 beamline), and DESY (PETRAIII, Hamburg, Germany; P11 beamline) for provision of synchrotron-radiation facilities and support during data collection.

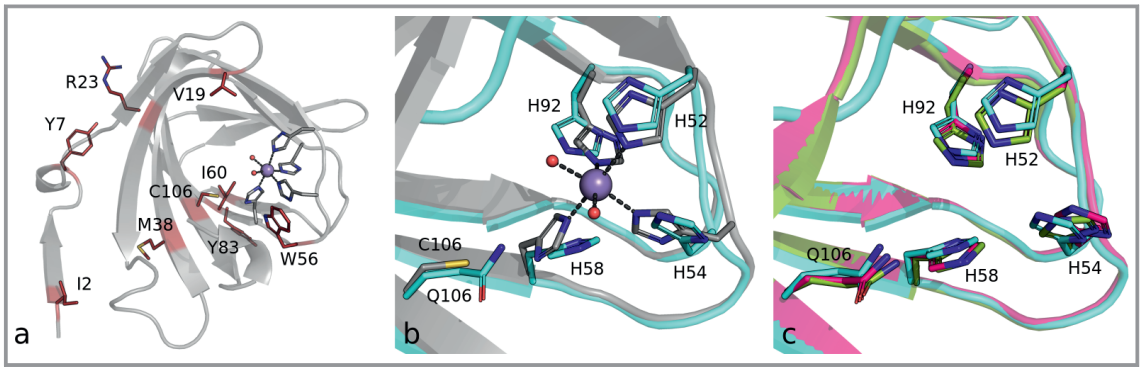

Figure 4. Structural characterisation of variants. a) All positions of amino acid exchanges of the best variants mapped on the TM1459 (PDB: 1VJ2). b) Superimposed active sites of TM1459 (PDB: 1VJ2, grey) and the C106Q variant (cyan). Manganese ion is shown as violet and water molecules as red spheres. c) Superposition of all three variant X-ray structures (TM1459-C106Q, cyan; TM1459-208, green; TM1459-AIFQ, magenta), showing very similar positions of histidine residues in the active site and no Mn bound. The figures were prepared using the program PyMOL.

Abbreviations

BSA	bovine serum albumin
CD	circular dichroism
CID	collision-induced dissociation
GC	gas chromatography
HPLC	high performance liquid chromatography
ICP-OES	inductively coupled plasma optical emission spectrometry
IPTG	isopropyl-beta-D-thiogalactopyranoside
Kan	kanamycin
KPi	potassium phosphate buffer
LB	lysogeny broth
LC	liquid chromatography
MES	2-(*N*-morpholino)ethanesulfonic acid
MS	mass spectrometry
NaPi	sodium phosphate buffer
PAR	4-(2-pyridylazo)resorcinol
PCR	polymerase chain reaction
PDB	Protein Data Base (www.rcsb.org)
SDS-PAGE	sodium dodecyl sulphate polyacrylamide gel electrophoresis
t-BuOOH	*tert*-butyl hydroperoxide
TTN	total turnover number

References

[1] A. L. Carroll, S. H. Desai, S. Atsumi, *Curr. Opin. Biotechnol.* **2016**, *37*, 8–15. DOI: https://doi.org/10.1016/j.copbio.2015.09.003

[2] B. R. Travis, R. S. Narayan, B. Borhan, *J. Am. Chem. Soc.* **2002**, *124 (15)*, 3824–3825. DOI: https://doi.org/10.1021/ja017295g

[3] A. Rajagopalan, B. Seisser, F. G. Mutti, M. Schober, W. Kroutil, *J. Mol. Catal. B: Enzym.* **2013**, *90*, 118–122. DOI: https://doi.org/10.1016/j.molcatb.2013.02.002

[4] A. Rajagopalan et al., *ChemBioChem* **2013**, *14 (18)*, 2427–2430. DOI: https://doi.org/10.1002/cbic.201300601

[5] I. Hajnal, K. Faber, H. Schwab, M. Hall, K. Steiner, *Adv. Synth. Catal.* **2015**, *357 (14–15)*, 3309–3316. DOI: https://doi.org/10.1002/adsc.201500608

[6] M. Fink, S. Trunk, M. Hall, H. Schwab, K. Steiner, *Front. Microbiol.* **2016**, *7*, 1511. DOI: https://doi.org/10.3389/fmicb.2016.01511

[7] B. S. Berlett, R. L. Levine, E. R. Stadtman, *J. Biol. Chem.* **1996**, *271 (8)*, 4177–4182. DOI: https://doi.org/10.1074/jbc.271.8.4177

[8] E. R. Stadtman, *Free Radical Biol. Med.* **1990**, *9 (4)*, 315–325. DOI: https://doi.org/10.1016/0891-5849(90)90006-5

[9] L. Fucci, C. N. Oliver, J. Coont, E. R. Stadtman, *Proc. Natl. Acad. Sci. U. S. A.* **1983**, *80 (6)*, 1521–1525. DOI: https://doi.org/10.1073/pnas.80.6.1521

[10] I. Verrastro, S. Pasha, K. T. Jensen, A. R. Pitt, C. M. Spickett, *Biomolecules* **2015**, *5 (2)*, 378–411. DOI: https://doi.org/10.3390/biom5020378

[11] E. Shacter, *Drug Metab. Rev.* **2000**, *32 (3–4)*, 307–326. DOI: https://doi.org/10.1081/DMR-100102336

[12] N. Fujieda, H. Ichihashi, M. Yuasa, Y. Nishikawa, G. Kurisu, S. Itoh, *Angew. Chem., Int. Ed.* **2020**, *59 (20)*, 7717–7720. DOI: https://doi.org/10.1002/anie.202000129

[13] N. Fujieda, T. Nakano, Y. Taniguchi, H. Ichihashi, H. Sugimoto, Y. Morimoto, Y. Nishikawa, G. Kurisu, S. Itoh, *J. Am. Chem. Soc.* **2017**, *139 (14)*, 5149–5155. DOI: https://doi.org/10.1021/jacs.7b00675

[14] M. Hogbom, *Mol. Cell. Proteomics* **2005**, *4 (6)*, 827–834. DOI: https://doi.org/10.1074/mcp.T400023-MCP200

[15] J. M. Mermet, *Anal. Chim. Acta* **1991**, *250*, 85–94. DOI: https://doi.org/10.1016/0003-2670(91)85064-Y

[16] W. Kabsch, *Acta Crystallogr., Sect. D: Biol. Crystallogr.* **2010**, *66 (2)*, 125–132. DOI: https://doi.org/10.1107/S0907444909047337

[17] A. J. McCoy, R. W. Grosse-Kunstleve, P. D. Adams, M. D. Winn, L. C. Storoni, R. J. Read, *J. Appl. Crystallogr.* **2007**, *40 (4)*, 658–674. DOI: https://doi.org/10.1107/S0021889807021206

[18] L. Jaroszewski et al., *Proteins* **2004**, *56 (3)*, 611–614. DOI: https://doi.org/10.1002/prot.20130

[19] P. V. Afonine, R. W. Grosse-Kunstleve, N. Echols, J. J. Headd, N. W. Moriarty, M. Mustyakimov, T. C. Terwilliger, A. Urzhumtsev, P. H. Zwart, P. D. Adams, *Acta Crystallogr., Sect. D: Biol. Crystallogr.* **2012**, *68 (4)*, 352–367. DOI: https://doi.org/10.1107/S0907444912001308

[20] D. Liebschner et al., *Acta Crystallogr., Sect. D: Struct. Biol.* **2019**, *75 (10)*, 861–877. DOI: https://doi.org/10.1107/S2059798319011471

[21] S. Amlathe, V. K. Gupta, *Analyst* **1990**, *115 (10)*, 1385–1387. DOI: https://doi.org/10.1039/an9901501385

[22] F. Frottin, A. Martinez, P. Peynot, S. Mitra, R. C. Holz, C. Giglione, T. Meinnel, *Mol. Cell. Proteomics* **2006**, *5 (12)*, 2336–2349. DOI: https://doi.org/10.1074/mcp.M600225-MCP200

